

SUPPLEMENTARY INFORMATION

A high throughput approach for analysis of cell nuclear deformability at single cell level

Menekse Ermis^{1,2}, Derya Akkaynak³, Pu Chen⁴, Utkan Demirci^{4,*}, and Vasif Hasirci^{1,2,5,*}

¹BIOMATEN, METU Centre of Excellence in Biomaterials and Tissue Engineering, 06800, Ankara, Turkey

²METU Department of Biomedical Engineering, 06800, Ankara, Turkey

³Department of Mechanical Engineering, Massachusetts Institute of Technology, 77 Massachusetts Avenue,

Cambridge, MA 02139, USA

⁴Bio-Acoustic-MEMS in Medicine (BAMM) Laboratory, Canary Centre at Stanford for Early Cancer Detection,

Department of Radiology, School of Medicine, Stanford University, Palo Alto, CA, 94304, USA

⁵METU Department of Biological Sciences, 06800, Ankara, Turkey

*vhasirci@metu.edu.tr, utkan@stanford.edu

SUPPLEMENTARY INFORMATION

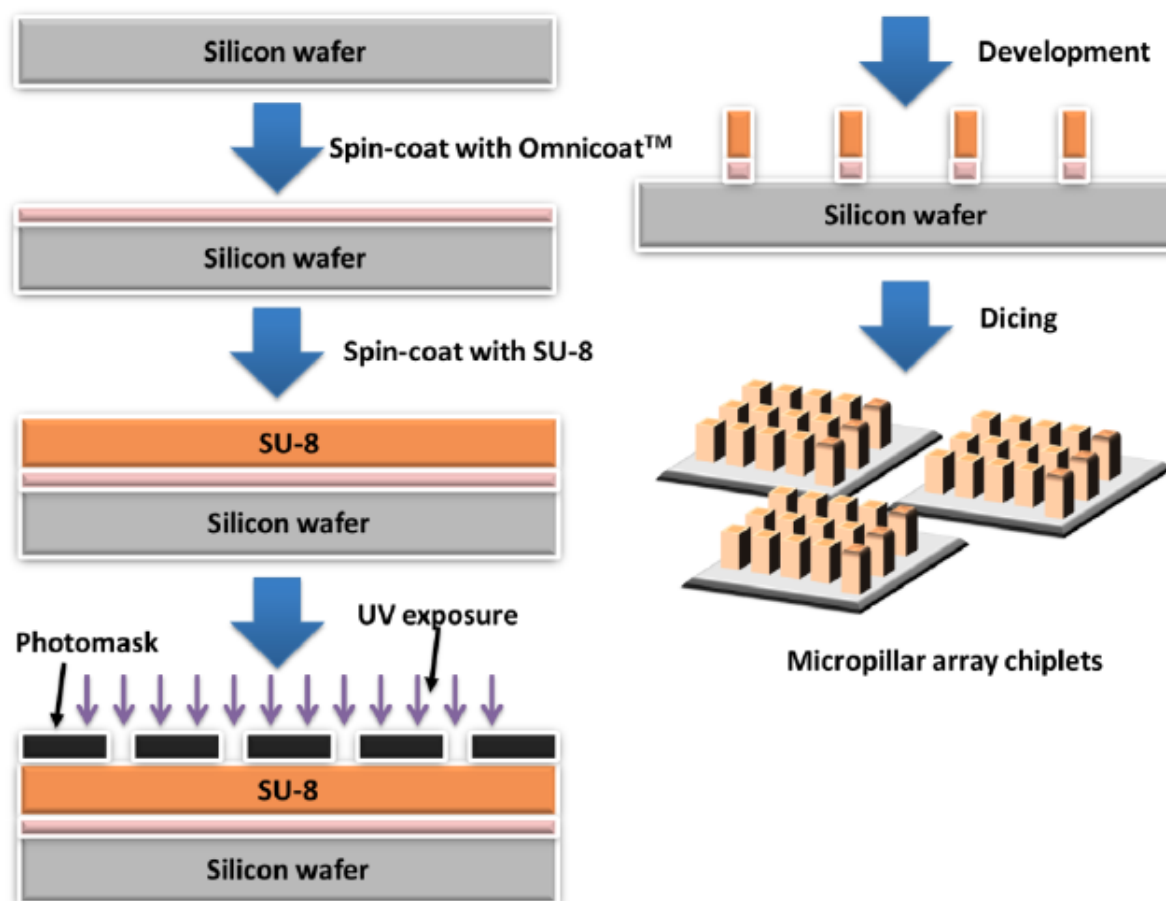
Tables

Supplementary Table 1: Examples of the methods to study cell and nuclear stiffness/deformability in the literature.

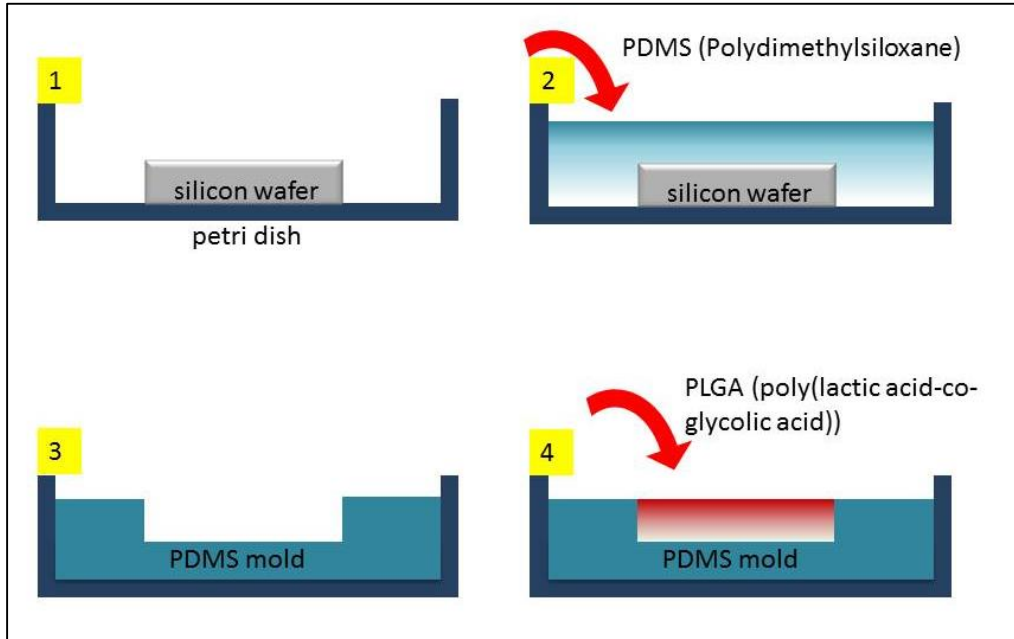
<i>Method</i>	<i>Cell type</i>	<i>Studied feature/structure</i>	<i>No of cells/ measurements</i>	<i>Ref.</i>
AFM indentation	Benign human breast epithelial cells (MCF-10A) Malignant human breast epithelial cells (MCF-7)	Global cell elasticity (Bulk Young's modulus)	<i>Not given in text</i>	28
PDMS microchannel-microfluidics device	Benign breast epithelial cells (MCF-10A) Non- metastatic tumor breast cells (MCF-7)	Elongation index, transit velocity in channel	50 cells	29
AFM indentation	Non-tumorigenic prostate cells (PZHPV-7) Prostatic adenocarcinoma (PC-3) Metastatic prostate carcinoma (Du 145) Metastatic prostate carcinoma (LNCaP) Normal mammary tissue (A184A1) Breast cancer (T47D) Breast adenocarcinoma (MCF7)	Global cell elasticity (Bulk Young's modulus)	232 indentation in 10x10 μm region	30
AFM indentation	Patient pleural effusion samples	Stiffness and adhesion	40 metastatic tumor cells 48 normal cells	31
Magnetic tweezers assay	Human ovarian cancer cell lines (OVCA429, IGROV, SKOV3, HEY, DOV13, OV2008 and Ovca420) Ovarian cancer stable cells lines (Ovca429Neo, Ovca429TbRIII)	Stiffness and compliance	<i>Not given in text</i>	32
AFM elastography	Primary neonatal rat alveolar type I and II cells	Elastic map of cells	30 cells, 121 indentations per cell	51
AFM indentation	Human neuroblastoma cells (SH-SY5Y)	Stiffness	<i>Cell number not given in text</i> , 36 indentations per cell	52
Hydrodynamic stretching	Patient pleural effusion samples Mouse embryonic stem cells (mESC) Human embryonic stem cells (hESC)	Cell deformability under hydrodynamic focusing	3427 mESC cells 2523 hECS cells	53
Micropipette aspiration	Human melanoma cell line (WM35) Metastatic melanoma cell line (Lu1205)	Nuclear deformation	66 WM 35 cells 45 Lu1250 cells	54

SUPPLEMENTARY INFORMATION

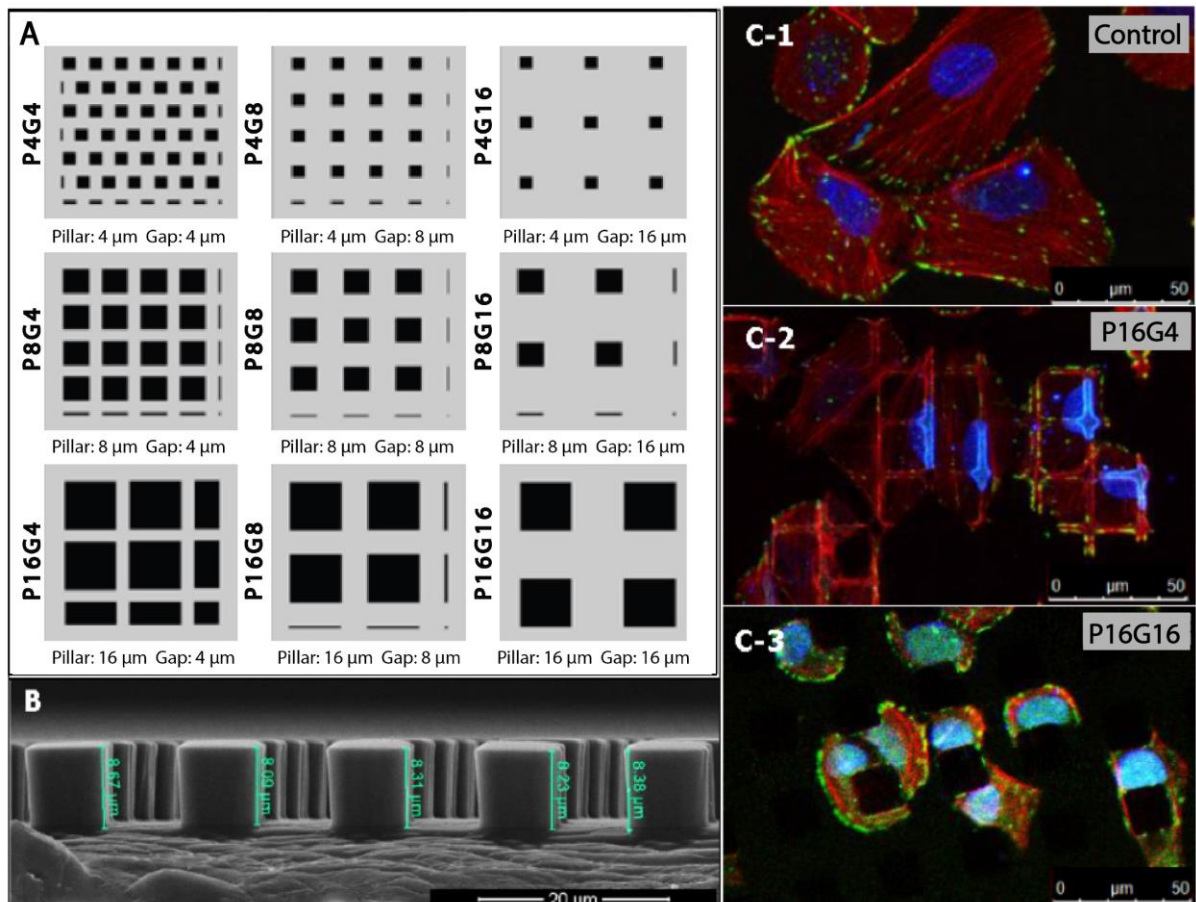
Figures



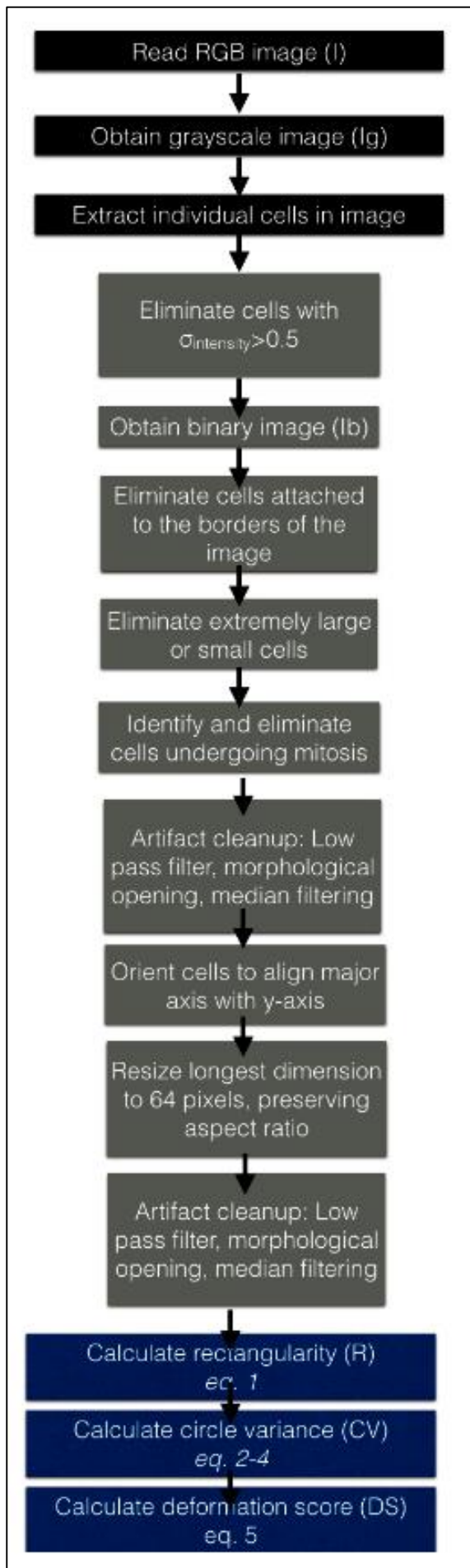
Supplementary Figure 1: Production of SU-8 micropillar array chip.



Supplementary Figure 2: Preparation of PDMS molds and poly(lactic acid-co-glycolic acid) (PLGA) (85:15) micropatterned films from SU-8 micropatterned array chiplets.



Supplementary Figure 3: Design of the micropillar array chip and the nucleus deformation response of Saos-2 cells to the various pillar and spacings. (a) The array, (b) SEM of a field on the surface (side view), and (c) deformation of Saos-2 nuclei of on some representative surfaces. (a) Top row consist of 4x4 μm pillars, from left to right spacing between the pillars are 4 μm , 8 μm , 16 μm . Middle row consist of 8x8 μm pillars, from left to right spacing between the pillars are 4 μm , 8 μm , 16 μm . Bottom row consists of 16x16 μm pillars, from left to right spacing between the pillars are 4 μm , 8 μm , 16 μm . (b) shows the side view of the pillars. Average pillar heights were determined as $8.3 \pm 0.2 \mu\text{m}$. (c1) Saos-2 osteosarcoma cells on Control surfaces show round-to-oval nuclei. (c2 and c3) Different levels of nuclear deformation were observed on P16G4 and P16G16, with more extensive deformation on the narrower gap (G4). Stains: Blue: nucleus/anti-LMNA, Red: cytoskeleton/Alexa-Phalloidin, Green: focal adhesions/anti-Paxillin).



Supplementary Figure 4: High-level flow of image processing algorithm.